DOI 10.1007/s10812-023-01547-1
Journal of Applied Spectroscopy, Vol. 90, No. 2, May, 2023 (Russian Original Vol. 90, No. 2, March–April, 2023)

LIGHT BEAM TRANSFORMATION AND MATERIAL DIAGNOSTICS BY DYNAMIC HOLOGRAPHY METHODS

A. L. Tolstik,* E. V. Ivakin, and I. G. Dadenkov UDC 535.34;548.4

Experimental results on frequency conversion of images by dynamic holograms and diagnostics of semiconductor materials and photorefractive and activated crystals based on the transient gratings method are presented. The possibility of visualization of infrared 3D images in real time is shown. Spectral regularities of short- (hundreds of microseconds) and long-lived (seconds) lattice recordings in photorefractive bismuth silicate crystals are established. The diffusion coefficient of excitation energy and the lifetime of excited states are measured. Techniques for compensation of induced anisotropy in active laser media and measurement of the thermal diffusivity coefficient of thin films and bulk thermoelectrics based on lead telluride are proposed.

Keywords: *dynamic holography, multi-wave mixing, spatially modulated spectroscopy, activated crystal, semiconductor, bismuth silicate, thermoelectric.*

Introduction. Work on holography was initiated by Boris Ivanovich Stepanov after the presentation in 1964 at the Institute of Physics, AS BSSR, of the candidate dissertation of Yu. N. Denisyuk, the founder of three-dimensional optical holography. A scientific group (and later a laboratory) on optical holography headed by A. S. Rubanov was formed in 1966. High-priority results were obtained for several years. The first steps were made via the transfer of ideas and methods of traditional (static) holography to dynamic recording and processing of light fields in nonlinear media. Attention was paid mainly to selection of photosensitive media. Considering the extensive experience of staff of the Institute of Physics with complicated organic compounds (dyes), efforts on recording holograms in transparent media were performed in 1970 and led to the discovery of a new physical phenomenon, i.e., conversion of a wave front (phase coupling) of light waves with four-wave mixing [1]. Then, the physical principles of dynamic holography were developed. Its close relationship with nonlinear optics was established. Methods using dynamic holograms for controlling the spatial structure of light beams and optical information processing and recording were developed. B. I. Stepanov, P. A. Apanasevich, E. V. Ivakin, and A. S. Rubanov were awarded a State Prize of the USSR for work in this area.

New pathways for solving problems with transformation of the space–time structure of light fields, transmission of images through inhomogeneous media, and the development of lasers with dynamic modes and powerful laser systems with wave-front conversion elements allowing the production of radiation with diffraction divergence and high spectral brightness were defined because of many studies of the optics of phase coupling in the 1980s. Research on dynamic holography was begun in the Department of Laser Physics and Spectroscopy, Belarusian State University (BSU), on the initiative of A. S. Rubanov. B. I. Stepanov was the first Head of the Department. The active collaboration of staff of the Institute of Physics and BSU led to the development and experimental confirmation of the theory of multi-wave mixing of laser radiation in resonant media [2], determination of the conditions for highly efficient transformation of light fields by volume holograms, and the development of methods for increasing the sensitivity for holographic recording at high rates. Optical bi- and multistability with four-wave mixing of light fields in resonant media was first analyzed in detail by numerical modeling methods [3] and was demonstrated by conversion of a wave front with simultaneous frequency doubling of a light wave [4]. A method for controlling the nonlinearity of multi-level resonant media using an additional light beam, the frequency of which was tuned to an induced absorption band from molecular excited states was proposed for increasing the diffraction efficiency of dynamic holograms.

*To whom correspondence should be addressed.

Belarusian State University, Minsk, Belarus; email: tolstik@bsu.by. Translated from Zhurnal Prikladnoi Spektroskopii, Vol. 90, No. 2, pp. 316–323, March–April, 2023. Original article submitted February 21, 2023; https://doi.org/10.47612/0514-7506-2023-90-2-316-323.

A new area of dynamic holography arose and used singular light beams (optical vortices) for recording. Research on multi-wave mixing in resonant media of singular light beams demonstrated the potential of using singular dynamic holograms to control the spatial and phase structure of laser radiation. Topological charge could be multiplied using various diffraction orders and frequency transformation of images and was promising for visualizing singular beams with a complicated topological structure and for coding information with an examination of the polarization and topological charge of a light beam as information parameters [5, 6].

The use of dynamic lattices to measure various parameters of nonlinear media was independently interesting. The expansion of the potential of diffraction methods for transforming light fields and methods of nonlinear spectroscopy is related to a transition to research on multi-wave mixings occurring in media with nonlinearities of the fifth and higher orders [7]. This situation occurs, e.g., in resonant media at intensities exceeding the saturation intensity. The dependence of a light-induced change of refractive index on intensity becomes nonlinear, leading to distortion of the lattice hatching profile, which ceases to be sinusoidal. Light scattering at various lattice Fourier harmonics determines diffraction in the second and higher orders. The signal wave phase is multiplied, which provides additional possibilities for controlling the light-beam wave front [8, 9]. The angular selectivity of a lattice allows waves diffracted in various orders to be independently reproduced by changing the direction of propagation of the reading wave or its frequency if the volume conditions of dynamic holograms is fulfilled [7]. The reading beam directed in Bragg mode at an angle corresponding to M-order diffraction is diffracted on the corresponding lattice spatial harmonic. Also, the diffraction efficiency into M-order can be related to the nonlinear susceptibility $\chi^{(2M+1)}$ and can lead to independent measurements of various orders of nonlinear susceptibility [10]. An analysis of the kinetics of the diffracted signal can identify the contributions of various types of nonlinearity, determine the recording mechanisms of dynamic lattices and the relaxation of nonlinear response, and measure the kinetic and thermal optical parameters of the materials [11, 12].

The method of dynamic lattices has features that give advantages over other optical diagnostic methods. For example, the dynamic lattice period being regulated and the clearly expressed direction of its vector can distinguish transport processes in the studied material from local photo-induced effects and find and study signatures of anisotropy in the samples. The coherence of the diffraction response of the sample to the laser action is also an important feature. Interference of the diffraction field with the coherent homodyne beam field ensures firstly, enhancement of the optical signal amplitude and secondly, identification and selection of its phase, which is especially important for the simultaneous involvement of many dynamic lattice mechanisms [13, 14]. Therefore, studies of recording of dynamic holograms and development on their basis of new methods for converting light fields and diagnosing materials are critical.

The present work reports experimental results for frequency conversion of images by dynamic holograms and diagnosis of semiconducting materials based on the method of dynamic lattices.

Frequency Conversion of 3D Images by Dynamic Holograms. Expansion of the capabilities of frequency conversion of light fields is associated with the use of nonlinear holographic recording. The condition for Bragg diffraction into higher orders was shown to occur if radiation of different frequencies was used for recording and reproduction of volume dynamic holograms in a nondegenerate multi-wave mixing scheme [7]. The dynamic lattice was recorded by signal E_S and reference E_1 waves of frequency ω (Fig. 1). The condition for Bragg diffraction into the M-order was observed to be fulfilled automatically for any direction of signal wave E_S for opposing propagation of the reference and reading waves ($M\mathbf{k}_1 + \mathbf{k}_2 = 0$) during reproduction of a hologram of wave E_2 at frequency $M\omega$. This allowed conversion of 3D images with an arbitrary wave front. Diffracted wave E_D had frequency $M\omega$ and propagated opposite to signal wave E_S ($\mathbf{k}_D = -M\mathbf{k}_S$).

Frequency conversion of images was previously achieved in a nondegenerate four-wave mixing scheme [10]. However, the propagation direction of the reading wave had to be selected to satisfy the phase synchronism condition $\mathbf{k}_D = \mathbf{k}_1 - \mathbf{k}_S + \mathbf{k}_2$. This limited the width of the angular spectrum of the reproduced image, allowing conversion of only the 2D image. By comparing the two schemes for converting light fields, it is noteworthy that although conversion of the wave front ($\varphi_D = -2\varphi_S$, $\mathbf{k}_D = -2\mathbf{k}_S$, $\omega_D = 2\omega$) occurred for multi-wave mixing, the retention of the phases ($\varphi_D = -\varphi_S$) as the frequency increased ($\omega_D = 2\omega$) for four-wave mixing meant that the spatial structure of the wave front was smoothed. For example, reproduction of a dynamic hologram at double the frequency in the four-wave mixing scheme for a divergent signal beam with a radius of curvature of the wave front R_0 led to generation of a convergent beam with double the radius of curvature $R \approx 2R_0$ while the diffracted wave was a convergent light beam with the same radius of curvature R_0 for six-wave mixing.

Bragg diffraction of laser radiation at double the frequency in an EtOH solution of polymethine dye No. 3274U was used to produce multi-wave mixing at a nondegenerate frequency. This dye has an absorption band at the fundamental

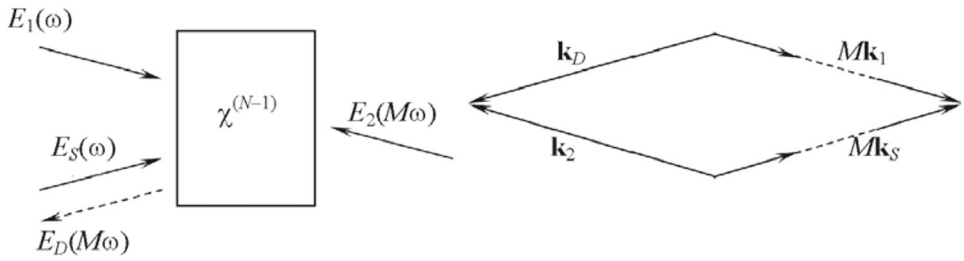

Fig. 1. Diagram of setup for frequency conversion of 3D images and corresponding diagram of wave vectors.

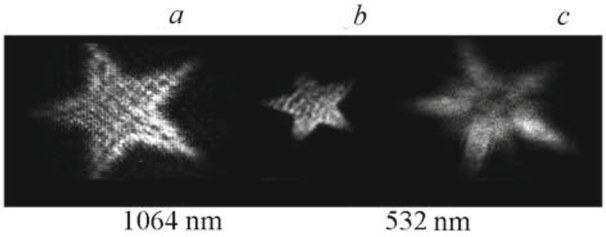

Fig. 2. Illustration of frequency conversion of images by dynamic holograms: starting image (a); images reproduced in four- and six-wave conversion (b, c).

generation frequency of yttrium aluminum garnet (λ = 1.064 μm) and is practically transparent at the second-harmonic frequency (λ = 532 nm). This allows dynamic holograms to be recorded in the IR spectral region and reproduced in the visible region (saturation intensity I_s = 13 MW/cm^2, lifetime of molecules in the excited singlet state, ~10 ps).

Figure 2 shows an example of image transformation from the IR to visible region [15]. Full frequency conversion of the images was observed for a six-wave mixing scheme while the geometric dimensions changed for four-wave mixing. Thus, multi-wave mixing methods under nonlinear dynamic hologram recording conditions enabled frequency conversion of complicated coherent images providing, e.g., visualization of IR images.

Recording Dynamic Holograms in Photorefractive Crystals of the Sillenite Family. Photorefractive crystals of the sillenite family that are broadband semiconductors (bismuth silicate and titanate are most popular) have the advantage of forming dynamic holograms in real time. Both continuous (mW) and pulsed (MW) laser radiation can be used to record holograms. The lifetime of the lattices can range from microseconds to hours [16–18]. Such features are due to redistribution of electrons in a spatially modulated radiation light field over defects and impurity trap centers in the band gap.

An optical parametric oscillator generating laser pulses of length 10 ms with the ability for smooth tuning of the generation wavelength in the range from 400 nm to 2 μm was used to analyze the spectral features for recording dynamic holograms in photorefractive crystals. The range 450–650 nm is optimal for photorefractive crystals of the sillenite family with pulsed recording. Use of the shorter wavelengths is limited by the anomalously high absorption as the wavelength of the direct interband transition is approached. Use of excitation at the longer wavelengths is inefficient because of the low absorption of sillenite crystals in the red spectral region.

Figure 3 shows oscillograms of the diffracted signal in bismuth silicate crystals that were obtained at two wavelengths of intensity ~1 MW/cm^2. A substantial dependence of the relaxation dynamics of the diffracted signal on wavelength of laser radiation and formation of dynamic lattices with equal relaxation times could be seen. A powerful short-lived lattice with relaxation time ~100 μs formed at λ = 460 nm. A long-lived lattice with relaxation time of the order of seconds played the main role for λ = 530 nm. Formation of the short-lived lattices could be attributed to a local nonlinearity mechanism and population of short-lived trap levels. The long-lived lattices formed via a diffusional nonlinearity mechanism and population of deeper traps. Use of the dynamic lattices method established the dependence of the contribution of each mechanism on the laser radiation wavelength. Short-lived lattices of lifetime ~100 μs in the blue–green region (430–500 nm) and long-lived lattices of lifetime of the order of hundreds of milliseconds to seconds in the red region (550–650 nm) were efficiently recorded.

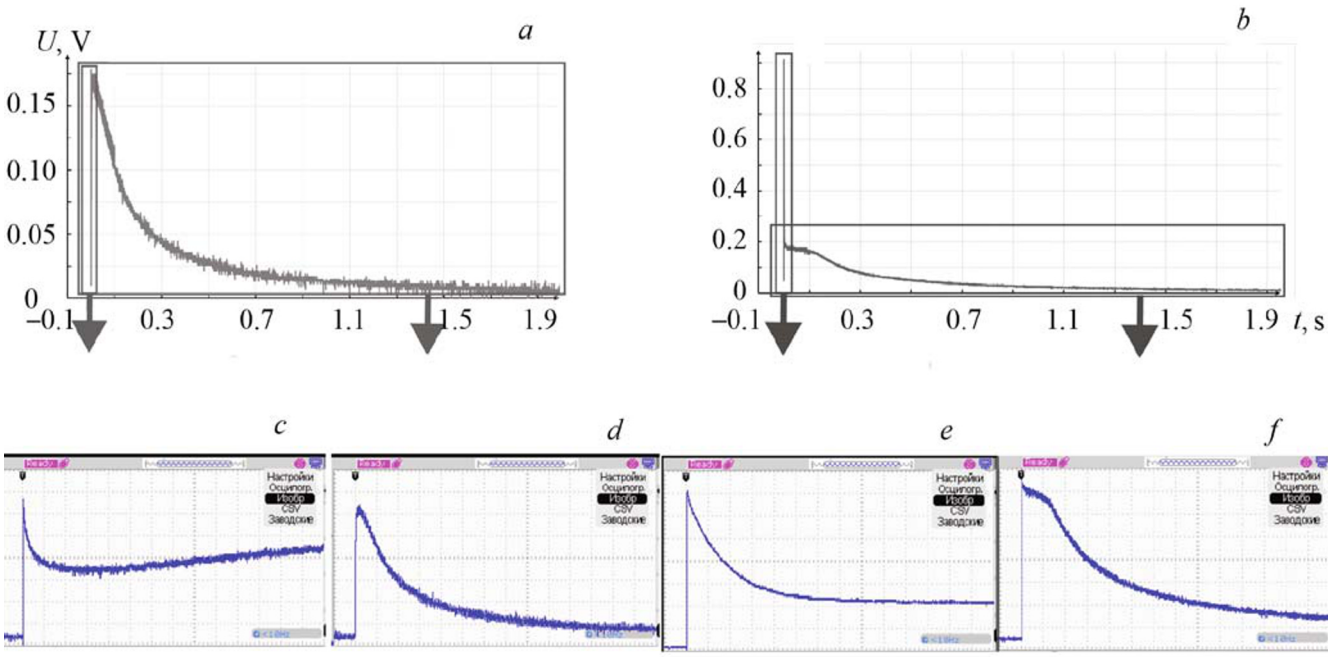

Fig. 3. Relaxation kinetics of dynamic lattices in bismuth silicate crystal at λ = 460 (a) and 530 nm (b) and corresponding oscillograms with scan time 50 μs (c, e) and 100 ms (d, f).

Use of Dynamic Lattices to Study the Properties of Laser Materials. Let us examine and quantitatively assess three regularities that are important from a practical viewpoint and appear in several laser materials, i.e., diffusion of excitation energy, re-emission effects, and anisotropy.

Spatial migration of excitation. Currently known energy-transfer effects between activator ions in laser crystals can simultaneously be associated with spatial migration of excitation. Modern trends toward miniaturization of active elements and increased activator concentrations are responsible for the urgency and growing interest in this problem. The diffusion coefficient of excitation energy D_E was directly measured by the high-frequency dynamic lattices method for a highly doped Yb^{3+}:GGG laser crystal [20], in contrast with indirect evaluation of it [19]. The equality $D_E = \Lambda^2/4\pi^2\tau$ was used to assess quantitatively the existence of diffusion in the direction of the dynamic lattice vector (excitation level gradient). Two dependences were plotted because the dynamic lattice period changed from 0.7 to 5 μm (Fig. 4). Diffusion coefficient D_E was determined from the slope of the approximation lines. According to the data, $D_E = 0.3 \cdot 10^{-8}$ cm^2/s at room temperature and increased to $1.2 \cdot 10^{-8}$ cm^2/s at 190°C. The intersection point of the lines with the ordinate ($\Lambda \to \infty$) gave the inverse lifetime of the metastable level in the crystal.

Neutralization of re-absorption of luminescence radiation. A dynamic lattice of the population of levels was recorded upon excitation of a laser crystal in the absorption band. Measurements of the lifetime of the metastable level over the lifetime of a dynamic lattice usually correspond closely to luminescence kinetic data. However, this was not observed for re-absorption of luminescence. The luminescence duration increased. The measurements had noticeable errors (Fig. 5). The method of dynamic lattices gave the true lifetime of the metastable level [21]. This was explained by the recording of the diffraction pattern of the excitation level being a coherent process while secondary random absorption of incoherent radiation in the crystal bulk could not affect the lifetime of the lattice of the excited level population and its diffraction efficiency.

Compensation of induced anisotropy. The efficiency of the thermal dynamic lattice changed and could decrease to zero in anisotropic crystals because of competition of the component changes of the refractive index Δn caused by thermal expansion of the material and mechanical stresses (Fig. 6). The total photoinduced refractive index of the material was observed to switch sign on passing through point *A*. The total change of the refractive index was equal to zero because of coupling of thermal and thermoelastic mechanisms of the change of refractive index. This allowed athermal directions compensating for the induced anisotropy to be selected.

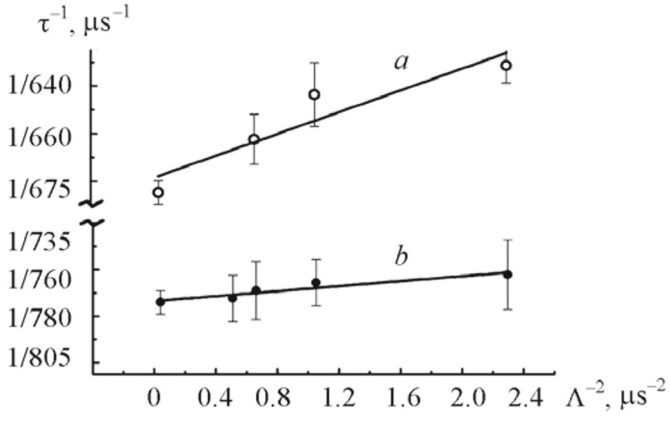

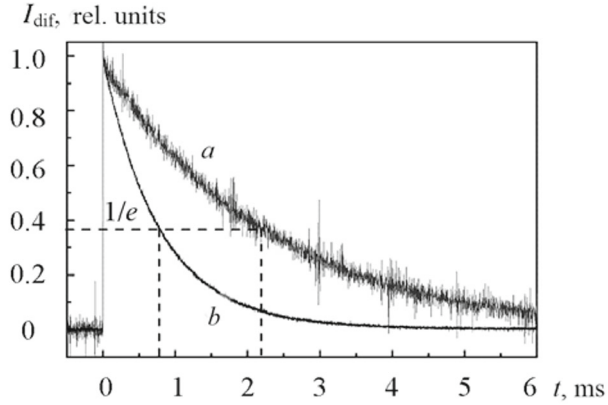

Fig. 4. Dependence of inverse lifetime of dynamic lattice τ in Yb^{3+}(21 at.%):GGG crystal on inverse square of its period Λ for sample temperature 190 (a) and 20ºC (b); λ_{ex} = 971 nm.

Fig. 5. Kinetics of luminescence (a) and diffraction signal (b) for Yb^{3+}:GGG laser crystal.

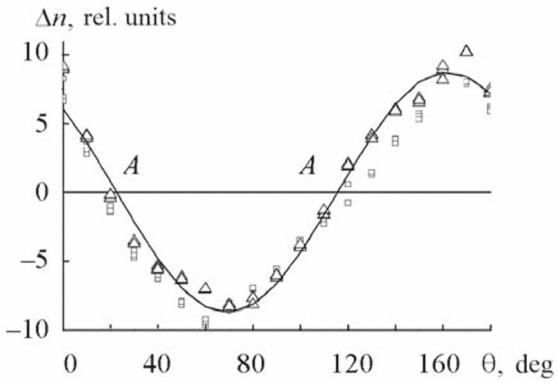

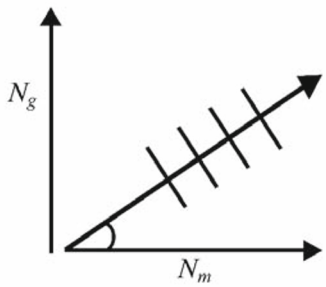

Fig. 6. Dependence of thermal contribution to induced photorefraction in anisotropic Yb:KYW crystal on angle between dynamic lattice vector and axis N_m; resulting thermal component Δn is absent at points A.

Study of Thermoelectrics Based on PbTe in the Bulk and Films. Compounds based on lead chalcogenides are known to be promising materials for thermoelectric applications [22, 23]. Maintenance of a high temperature gradient achieved because of low thermal conductivity is an important factor for reaching high efficiency of thermoelectrics. Also, a transition from bulk structures to thin films is known to facilitate a reduction of their thermal conductivity. Thus, studies of thermal transport in bulk and thin-film nanostructures of lead chalcogenides are crucial.

The penetration depth of probe radiation into PbTe for λ_{ex} = 532 nm is ≤20 nm. Therefore, the studies featured a determination of the surface thermal conductivity. The samples were thin films of the order of microns of the semiconductor PbTe with dopants of Sb and Bi that were deposited on glass or mice surfaces. Considering that the signal diffraction was formed simultaneously by three types of surface lattices (phase relief and phase and amplitude lattices of thermal conversion), an additional stationary lattice (homodyne) was used and allowed phase selection of the diffraction signal kinetics by addition of the homodyne field to the coherent diffraction field [24].

Figure 7a shows the three diffraction signals excited and relaxing simultaneously. Recorded signals of a different physical nature were selected and amplified because of the involvement of the coherent homodyne field with a controlled phase. The kinetics (1) described the total diffraction of the probe beam on the lattice relief formed on the film surface

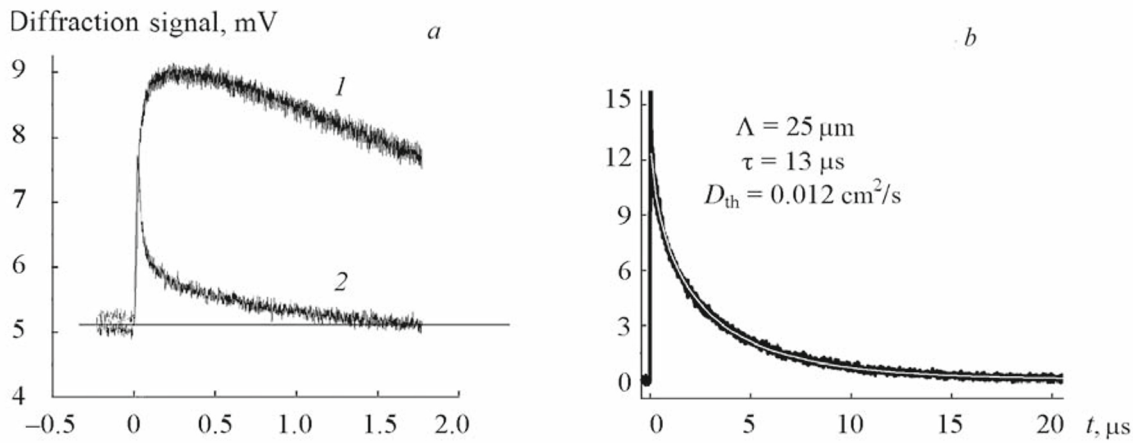

Fig. 7. Diffraction signals in PbTe:Sb film of thickness 6 μm on glass (lattice period 25 μm): initial diffraction fragments, phase shift of homodyne field relative to diffraction field 0 (1) and π/2 (2); line at 5 mV is intensity of homodyne beam (a); total diffraction kinetics of probe beam on phase of surface-relief lattice (b).

because of its heating and on the thermal conversion phase lattice. The phases of these two lattices opposed each other. Therefore, their resulting kinetics (1) contained a transitional section from 0 to 0.4 μs. This time interval was excluded from examination during analysis of the diffraction signal in general to minimize its role in forming the kinetics. The kinetics (2) determined the amplitude of the thermal conversion lattice surface shifted in phase by π/2 relative to the lattice phase (1). Its decay was observed to be significantly faster than the relief lattice. Figure 7b shown the total diffraction signal in the phase lattice of the surface relief. The decay of the thermal dynamic lattice was due to both horizontal heat transfer and to outflow of heat into the film according to the directions of the created temperature gradient. Assuming that heat transfer in both directions occurred at the same rate, the decaying diffraction signals were simulated by the additional error function $H(t) = H(0)\,\mathrm{Erfc}\,(t/\tau)^{1/2}$ [25]. Thus, the lifetime of thermal lattice τ was determined. Figure 7b compares theoretical (line inside the recorded kinetics) and experimental results. The thermal diffusivity D_{th} was calculated from the equality $D_{th} = \Lambda^2/4\pi^2\tau$ using the measured lattice period Λ and its lifetime τ.

The experimental studies using the dynamic lattices method demonstrated the efficiency of applying them to monitoring the properties of both bulk and film materials. The ability to control the direction and magnitude of the excitation gradient allowed the anisotropy of the sample physical parameters to be studied and transport effects of heat-, mass-, and energy-transfer, etc. to be monitored. The use of the coherent nature of the diffraction signal together with the coherent homodyne field played a positive role in the studies of the optical materials. This allowed the amplification and filtration of useful signals and increased the information value of the experimental results.

Conclusions. Regularities in the recording of dynamic lattices with different relaxation times in photorefractive crystals used in highly sensitive adaptive interferometry systems were established based on the developed methods of contact-free diagnostic methods for functional materials. The directions in which compensation of thermo-optical distortions occurred were selected to analyze photoinduced processes in activated crystals. The unique capabilities to measure the thermal conductivity coefficient of thin-film materials were demonstrated using thermoelectrics as examples.

REFERENCES

1. B. I. Stepanov, E. V. Ivakin, and A. S. Rubanov, *Dokl. Akad. Nauk SSSR*, **196**, No. 3, 567–571 (1971).
2. A. L. Tolstik, *Multi-wave Mixings in Solutions of Complicated Organic Compounds* [in Russian], BGU, Minsk (2002).
3. V. V. Kabanov, A. S. Rubanov, A. L. Tolstik, and A. V. Chaley, *Opt. Commun.*, **71**, No. 3–4, 219–223 (1989).
4. S. M. Karpuk, A. S. Rubanov, and A. L. Tolstik, *Opt. Spectrosc.*, **80**, No. 2, 276–280 (1996).
5. O. G. Romanov, D. V. Gorbach, and A. L. Tolstik, *Opt. Spectrosc.*, **115**, No. 3, 335–339 (2013).
6. A. L. Tolstik, *Russ. Phys. J.*, **58**, No. 10, 1431–1440 (2016).
7. A. S. Rubanov, A. L. Tolstik, S. M. Karpuk, and O. Ormachea, *Opt. Commun.*, **181**, Nos. 1–3, 183–190 (2000).

8. A. L. Tolstik, *Proc. SPIE*, **3684**, 110–117 (1998).
9. O. G. Romanov and A. L. Tolstik, *J. Appl. Spectrosc.*, **76**, No. 3, 370–376 (2009).
10. A. Tolstik, *Proc. SPIE*, **3580**, 73–80 (1998).
11. E. V. Ivakin, A. V. Sukhadolau, O. L. Antipov, and N. V. Kuleshov, *Appl. Phys. B*, **86**, No. 2, 315–318 (2007).
12. E. V. Ivakin, A. V. Sukhadolau, V. G. Ralchenko, A. V. Vlasov, and A. V. Homich, *Quantum Electron.*, **32**, No. 4, 367–372 (2002).
13. J. A. Johnson, A. A. Maznev, K. A. Nelson, M. T. Bulsara, E. A. Fitzgerald, T. C. Harman, S. Calawa, C. J. Vineis, and G. Turner, *J. Appl. Phys.*, **111**, Article ID 023503 (1–7) (2012).
14. A. Tolstik, I. Dadenkov, and A. Stankevich, *J. Opt. Technol.*, **89**, No. 5, 250–254 (2022).
15. O. Ormachea, O. G. Romanov, A. L. Tolstik, J. L. Arce-Diego, F. Fanjul-Velez, and D. Pereda-Cubian, *Opt. Express*, **14**, No. 18, 8298–8304 (2006).
16. A. L. Tolstik, A. Yu. Matusevich, M. G. Kisteneva, S. M. Shandarov, S. I. Itkin, A. E. Mandel′, Yu. F. Kargin, Yu. N. Kul′chin, and R. V. Romashko, *Quantum Electron.*, **37**, No. 11, 1027–1032 (2007).
17. A. Matusevich, A. Tolstik, M. Kisteneva, S. Shandarov, V. Matusevich, A. Kiessling, and R. Kowarschik, *Appl. Phys. B: Lasers Opt.*, **92**, No. 2, 219–224 (2008).
18. I. G. Dadenkov, A. L. Tolstik, Yu. I. Miksyuk, and K. A. Saechnikov, *Opt. Spectrosc.*, **128**, No. 9, 1401–1406 (2020).
19. L. Meilhac, G. Pauliat, and G. Roosen, *Opt. Commun.*, **203**, Nos. 3–6, 341–347 (2002).
20. I. G. Kisialiou and E. V. Ivakin, *J. Appl. Spectrosc.*, **81**, No. 6, 978–982 (2015).
21. I. G. Kisialiou, *Appl. Opt.*, **51**, No. 22, 5458–5463 (2012).
22. A. V. Dmitriev and I. P. Zvyagin, *Phys. Usp.*, **53**, No. 8, 789–803 (2010).
23. I. Lubomirsky and O. Stafsudd, *Rev. Sci. Instrum.*, **83**, No. 5, Article ID 051101 (1–18) (2012).
24. E. V. Ivakin, A. L. Tolstik, D. V. Gorbach, and A. A. Stankevich, *J. Eng. Phys. Thermophys.*, **95**, No. 4, 1026–1030 (2022).
25. O. W. Kading, H. Skurk, A. A. Maznev, and E. Matthias, *Appl. Phys. A: Mater. Sci. Process.*, **61**, No. 3, 253–261 (1995).